Preprints, 22nd Conf. Severe Local Storms (2004)
Hyannis, MA, Amer. Meteor. Soc., CD-ROM, 13.6

13.6 GROWTH OF CIRCULATION AROUND SUPERCELL UPDRAFTS

Robert Davies-Jones*
National Severe Storms Laboratory, NOAA
Norman, Oklahoma

1. INTRODUCTION

Are the physical processes that cause updraft rotation and propagation in isolated supercells storms the same in all types of shear? Are they always due primarily to the *nonlinear* interaction between the updraft and environmental shear? Or are they due mainly to this *nonlinear* interaction when the hodograph is *nearly straight* and due mostly to the *linear* updraft-shear interaction when the hodograph is *highly curved*?

This paper, which is a summary of Davies-Jones (2004; hereafter DJ04), addresses these questions. In DJ04, a formula is derived for the rate of change of circulation around an updraft perimeter at a given level. This quantity depends on the motion of points on the edge (the zero contour of vertical velocity). Thus, DJ04 also obtained a formula for propagation of an updraft edge by using Petterssen's formula for the motion of an isopleth and replacing the vertical-velocity tendency with the advection of vertical velocity and the vertical force. Previously, Davies-Jones (2002a,b; hereafter DJ02) had obtained a formula that quantified propagation of an updraft maximum at a given height.

Propagation of the edge and growth of circulation around the edge both depend on the vertical force, which in inviscid anelastic flow is simply the local nonhydrostatic vertical pressure gradient force (NHVPGF) in the non-Archimedean formulation of the governing equations. We partition nonhydrostatic pressure into a linear mass-induced part, a linear shear-induced part, a nonlinear splat-induced part, and a nonlinear rotationally (or spin-) induced part, which are forced in the Poisson equation for nonhydrostatic pressure by the mass field, the linear interaction between the updraft and the environmental shear, the nonlinear 'splat' terms, and the nonlinear 'spin' terms, respectively. We use this partition to divide NHVPGF and local edge propagation into mass-, shear-, splat-, and rotationally induced components so that we can identify key processes. We also label circulation growth as linear or nonlinear according to whether the linear or the nonlinear NHVPGF plays the larger role in the development of updraft rotation. We examine published simulations of right-moving supercells in different types of shear and identify in each case whether the dominant mechanisms at 3 km height are linear or nonlinear from contour plots of variables at a single instant in time.

*Corresponding author address: Robert Davies-Jones, National Severe Storms Laboratory, NOAA, 1313 Halley Circle, Norman, Oklahoma 73069-8493.
e-mail: Bob.Davies-Jones@noaa.gov

2. MOTION OF A CLOSED CONTOUR

According to Petterssen's formula (Stewart 1945), an isopleth of vertical velocity w in a horizontal plane moves normal to itself (in the direction of the unit vector $\mathbf{n}$) at a point Q on the contour with the velocity

$$\mathbf{c}\bullet\mathbf{n}\big|_Q = \left.\frac{\partial w/\partial t}{-\partial w/\partial n}\right|_Q \tag{2.1}$$

where t is time and $\partial/\partial n \equiv \mathbf{n}\bullet\nabla$. Motion in the tangential direction is of no interest, as it does not move the contour.

The propagation (or nonadvective) velocity of the contour at Q is defined by

$$\mathbf{P}\bullet\mathbf{n}\big|_Q = \mathbf{c}\bullet\mathbf{n}\big|_Q - \mathbf{v}\bullet\mathbf{n}\big|_Q \tag{2.2}$$

where $\mathbf{v}$ is the wind. The inviscid, anelastic vertical-momentum equation for flow in supercells is

$$\frac{\partial w}{\partial t} = -\mathbf{v}_H\bullet\nabla_H w - w\frac{\partial w}{\partial z} - \alpha_s\frac{\partial p_{nh}}{\partial z} \tag{2.3}$$

where z is height above the ground (assumed flat), subscript H denotes horizontal, $\alpha_s(z)$ is the specific volume of the reference atmosphere, p_{nh} is the local nonhydrostatic pressure (or pressure p minus the local hydrostatic pressure p_h, which includes the weight of hydrometeors), and $-\alpha_s\partial p_{nh}/\partial z$ is the NHVPGF. Substituting for $\partial w/\partial t$ in (2.1) from (2.3) and using (2.2) yields

$$\mathbf{P}\bullet\mathbf{n}\big|_Q = \left.\frac{-\alpha_s\partial p_{nh}/\partial z}{-\partial w/\partial n}\right|_Q \tag{2.4}$$

for the propagation of the updraft perimeter (closed $w=0$ contour with outward unit normal $\mathbf{n}$). The updraft edge propagates outward (inward) on its side of upward (downward) NHVPGF (Fig. 1; Rotunno and Klemp 1982).

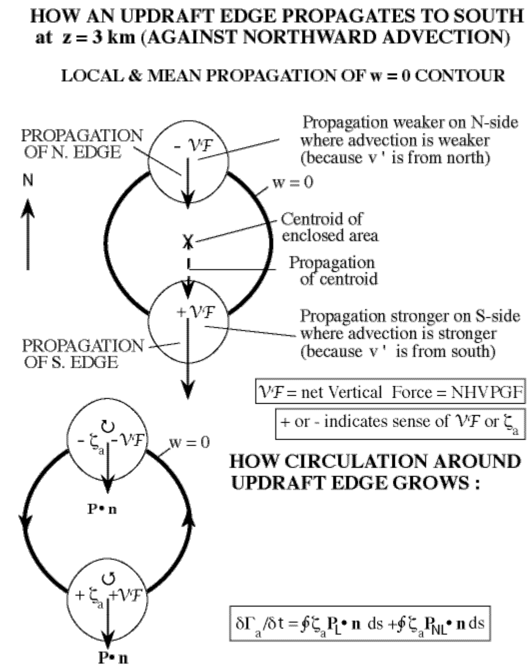

FIG. 1. Illustrations showing how an updraft edge propagates and how an updraft acquires cyclonic circulation. Symbols are defined in the text.

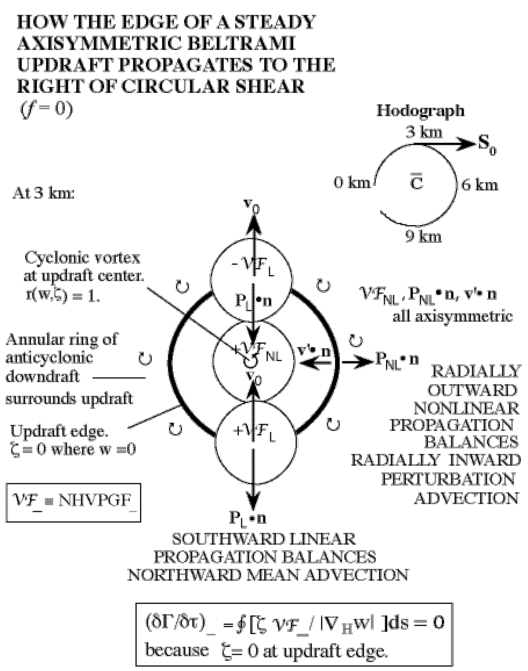

FIG. 2. Diagram showing how a cyclonic Beltrami updraft propagates 90 to the right of the shear vector $\mathbf{S}_0$. Symbols are defined in the text.

DJ04 also obtained a formula for the motion of the updraft centroid (i.e., the centroid of the area enclosed by the $w = 0$ contour). The motion $\bar{\mathbf{c}}$ (propagation velocity $\bar{\mathbf{P}}$) of the centroid is a weighted average of the outward motions (propagations) of the points on the updraft's edge. The weight function is the position vector from the centroid to each point.

3. CIRCULATION-GROWTH FORMULA

It is shown in DJ04 that the rate of change of the absolute circulation, $\Gamma_a \equiv \oint_{L(t)} \mathbf{v}_a \bullet d\mathbf{x}$, around an updraft edge $L(t)$ on a f-plane is

$$\frac{\delta\Gamma_a}{\delta t} = \oint_{L(t)} \frac{\partial \mathbf{v}_H}{\partial t} \bullet d\mathbf{x} + \oint_{L(t)} \zeta_a \mathbf{c} \bullet \mathbf{n} ds \qquad (3.1)$$

where $\mathbf{v}_a$ is the absolute wind, $\mathbf{x} \equiv (x, y, z)$ is the position vector, $\zeta_a \equiv \zeta + f$ is the vertical component of the absolute vorticity $\boldsymbol{\omega}_a$, and ds is the element of arc length along the edge. Substituting for $\partial \mathbf{v}_H / \partial t$ from the inviscid anelastic equation for horizontal motion

$$\partial \mathbf{v}_H / \partial t = -\nabla_H (\mathbf{v} \bullet \mathbf{v}/2) + (\mathbf{v} \times \boldsymbol{\omega}_a)_H - \alpha_s \nabla_H p$$

and simplifying gives us (3.2)

$$\frac{\delta\Gamma_a}{\delta t} = \oint_{L(t)} \zeta_a \mathbf{P} \bullet \mathbf{n} ds. \qquad (3.3)$$

At a given height in inviscid anelastic flow, the rate of gain in updraft circulation is equal to the net non-advective flux of cyclonic vorticity through the moving updraft edge into the updraft. To increase its circulation, the updraft must propagate. Generation of cyclonic circulation requires the edge to propagate outward on its cyclonic side and/or inward on its anticyclonic side (Fig. 1). [Note that updrafts shed as well as gather vorticity.]

4. LINEAR AND NONLINEAR PROPAGATION AND CIRCULATION GROWTH

In an anelastic system, nonhydrostatic pressure is obtained as the solution of a Poisson equation. Thus, p_{nh} satisfies the boundary-value problem

$$\begin{aligned} -\nabla^2 p_{nh} &= F = F_{\mathrm{M}} + F_{\mathrm{L}} + F_{\mathrm{NL}}, \\ \partial_z p_{nh} &= 0 \text{ at } z = 0 \end{aligned} \qquad (4.1)$$

where $F_{\mathrm{M}} = g\nabla_H^2 \mathfrak{M}$, $F_{\mathrm{L}} = 2\rho_s \mathbf{S}_0 \bullet \nabla_H w$, and F_{NL} is the nonlinear forcing (DJ02). Here $\mathfrak{M}$ is the mass of air and hydrometeors in the overlying column, $\rho_s(z) \equiv \alpha_s^{-1}$ is the reference air density,

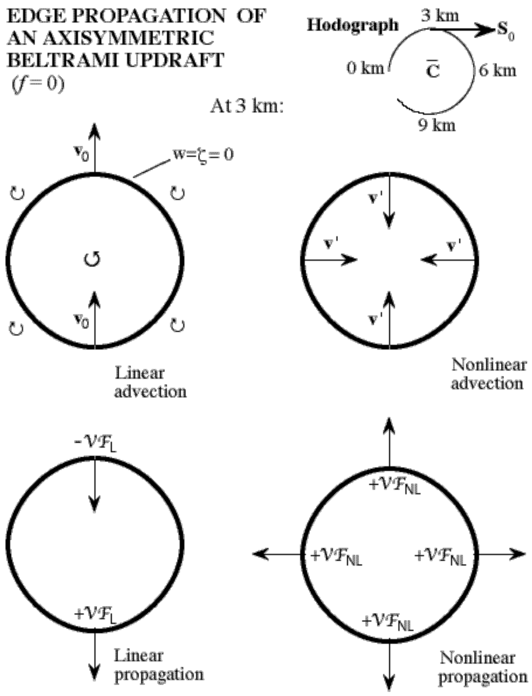

FIG. 3. The balance between linear (nonlinear) advection and linear (nonlinear) propagation at the edge of an axisymmetric Beltrami updraft in circular veering shear.

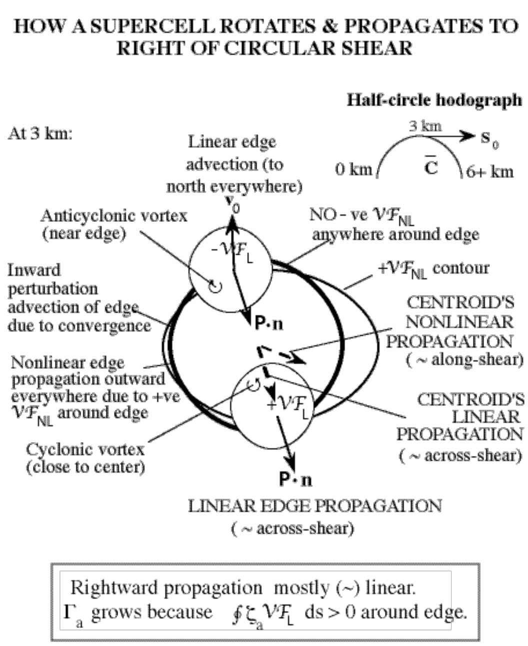

FIG. 4. Illustration of how a supercell in circular shear acquires circulation and propagates to the right of the shear through mainly linear mechanisms.

$\mathbf{S}_0 \equiv d\mathbf{v}_0/dz$ is the environmental shear, and $\mathbf{v}_0$ is the environmental wind. F_{NL} is the sum of F''_{SPLAT}, a positive- definite "splat" term equal to ρ_s times the nonlinear part of the squared total deformation, and F''_{SPIN}, a negative-definite "spin" term equal to $-\rho_s/2$ times the square of the perturbation vorticity $\boldsymbol{\omega}'$ plus the small Coriolis-induced forcing ($-\rho_s f\zeta$). The linear Coriolis term is included in the nonlinear spin term to keep the explicit spin terms together. [Linear splat and earth-relative spin terms are the implicit parts of F_{L}.] Splat (spin) forcing acts at a distance to raise (lower) pressure (DJ02).

The solution p_{nh} of (4.1) may be decomposed into mass-induced (M), shear-induced (L), and nonlinear (NL) parts corresponding to the various forcing terms. The nonlinear part consists of splat-induced (S) and rotationally induced (R) pieces. The formal solution of (4.1) by the method of images is

$$p_{nh\_}(\mathbf{x}) = \int_{-\infty}^{\infty}\int_{-\infty}^{\infty}\int_{-\infty}^{\infty} G(\hat{\mathbf{x}},\mathbf{x})F_{\_}(\hat{\mathbf{x}})d\hat{\mathbf{x}} \qquad (4.2)$$

where subscript _ stands for M, L, NL, R, or S, $G(\hat{\mathbf{x}},\mathbf{x}) = 1/4\pi|\hat{\mathbf{x}}-\mathbf{x}|$ is the Green's function, and the forcing function is extended evenly below the ground [$F_{\_}(x,y,-z) = F_{\_}(x,y,z)$].

By inserting $p_{nh} = p_{nh\,\mathrm{M}} + p_{nh\,\mathrm{L}} + p_{nh\,\mathrm{NL}}$ into (2.4), we also decompose local propagation of the edge $\mathbf{P}\bullet\mathbf{n}$ into a linear mass-induced part, a linear shear-induced part owing to the interaction of the updraft with the environmental shear, and nonlinear splat- and spin-induced parts. Propagation owing to nonlinear spin forcing is called rotationally induced propagation (Klemp 1987; hereafter K87). Introducing this decomposition into (3.3) similarly partitions the circulation gain around the edge into linear and nonlinear parts (see equation in Fig. 1).

5. TEST OF FORMULAS

A steady non-buoyant Beltrami updraft in a homentropic (constant-entropy) environment with circular shear (i.e., with a hodograph comprised of an arc that subtends an angle of $\sim 180^{\circ}$ or more at the center of curvature) provides an exact solution of the governing equations for testing formulas (2.4) and (3.3). Since the flow is steady, the formulas should predict no edge motion and no gain in circulation. There is no mass-induced propagation because the flow has no horizontal density gradients. In DJ04, it is shown that, at each point on the updraft perimeter, the tendency for the environmental (perturbed) flow to advect the edge normal to itself is exactly offset by linear (nonlinear) propagation in the opposite direction. When the Beltrami updraft is axisymmetric, the nonlinear propagation and advection are also axisymmetric and individually only affect the updraft radius, not the position of its center (Figs. 2 and 3). The edge does not move because advection exactly cancels propagation. The propagation of the updraft off the hodograph is entirely linear (Figs. 2, 3: DJ04). There is no non-advective flux of vertical vorticity into the updraft because $\zeta = 0$ at the edge. Therefore, the circulation of the updraft does not change.

6. EXAMPLE OF LINEAR CIRCULATION GROWTH

Armed with the above tools, we can now deduce the mechanisms for edge propagation and circulation growth in numerically simulated supercells. Schematic figures 3-6 summarize the main features of right-moving storms at 40 min after initiation in the simulations of Weisman and Rotunno (2000; hereafter WR).

In an environment with moderate CAPE and a semi-circle hodograph, the right-moving updraft in a numerical simulation resembles an axisymmetric Beltrami updraft in many aspects (Fig. 4; DJ02) even though buoyancy torques in the simulated storm generate appreciable baroclinic vorticity, which precludes a pure Beltrami flow (BF). The storm motion is slightly northeast of the hodograph's center of curvature and at 3 km the right-moving updraft is propagating off the hodograph to the south-southeast (SSE). For the corresponding inviscid, steady BF, the motion vector is at the center and the propagation is to the south or 90° to the right of the shear vector (Figs. 2, 3). The cross section of the updraft is quite circular as in the BF. The correlation coefficient between vertical velocity and vertical vorticity at 3 km is 0.7 compared to 1 for the BF. The cyclonic vortex is close to but on the south side of the updraft center where its suction helps to maintain the updraft, while the anticyclonic vortex is on the northern edge (Fig. 4). This is quite similar to the BF, where the cyclonic vortex is collocated with the updraft and the anticyclonic vorticity is in the surrounding concentric downdraft (Fig. 2). Positive linear NHVPGF on the SSE side is moving the SSE edge of the updraft to the SSE and the negative linear NHVPGF on the north-northwest (NNW) side is moving the NNW edge to the SSE (Fig. 4). Thus linear propagation is opposing the advection of the updraft centroid by the storm-relative environmental wind. In the BF, the positive and negative linear NHVPGF are on the south and north sides, respectively, so the linear propagation of the centroid is to the south rather than SSE, and exactly negates northward advection of the centroid by the updraft-relative environmental wind (Figs. 2, 3).

The nonlinear NHVPGF is upward all around the edge as in the BF and thus acts mainly to expand the updraft outward on all sides (Fig. 4). Its distribution has a lesser effect on rightward centroid propagation than the more asymmetric distribution of the smaller linear NHVPGF. In the BF, updraft expansion owing to nonlinear propagation exactly balances contraction owing to inward advection by convergent perturbation flow. The axisymmetry of the wind deviation $\mathbf{v}'$ and nonlinear pressure p_{NL} prevents nonlinear propagation of the updraft centroid (Figs. 2, 3). In both flows, none of the nonlinear propagation is associated with decay of the north edge of the updraft. In the simulated storm, the difference in outward nonlinear propagation on opposite sides of the updraft is most pronounced in the east-west direction, indicating that nonlinear propagation of the centroid is mainly eastward or along the shear (Fig. 4). Thus the southward (rightward) component of centroid propagation is predominantly linear.

Beltrami flows cannot shed light on how circulation develops in circular shear because there is no amplifying Beltrami solution. Around the edge of the simulated updraft the average product of vertical vorticity and nonlinear NHVPGF is small. Thus, the combination of upward linear NHVPGF on the cyclonic part of the edge and downward linear NHVPGF on the anticyclonic part indicates that the circulation is growing primarily linearly at this time (Fig. 4). A significant positive contribution to $\delta\Gamma/\delta t$ is associated with the collocation of anticyclonic vorticity with negative linear NHVPGF on the northern side of the updraft edge. Lemon (1976) observed similar behavior in a storm in quasi-circular low-level shear. He detected increasing cyclonic updraft rotation as an updraft shed an anticyclonic eddy on its north side.

The fact that the propagation of simulated buoyant updrafts in circular shear is mainly linear and hence quite Beltrami like does not imply that the simulated updrafts are Beltrami flows. It just means that predominantly linear propagation is not restricted to BFs and can still occur in flows with moderate buoyancy and imperfect alignment of vortex lines and streamlines. The axisymmetric Beltrami updraft in circular shear merely serves as the limiting case where the

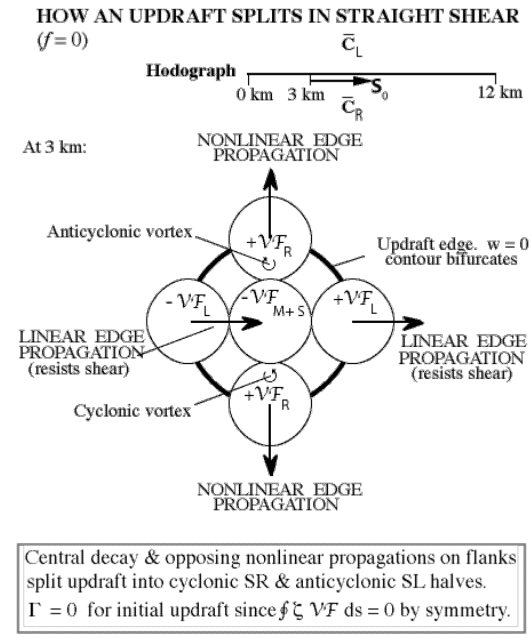

FIG. 5. Schematic demonstrating how an updraft splits in strong unidirectional shear. Here $\bar{c}_L$ and $\bar{c}_R$ are the storm motions of the subsequent SL and SR supercells.

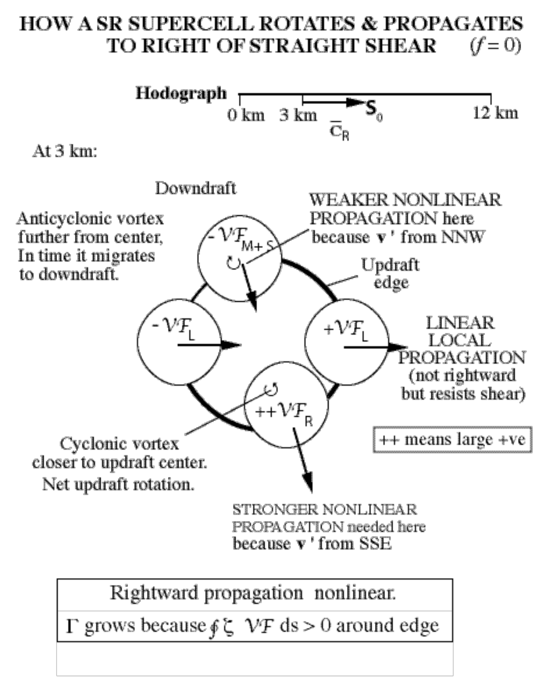

FIG. 6. Diagram showing how the SR supercell updraft in unidirectional shear continues to propagate to the right and to rotate cyclonically long after storm splitting.

propagation off a curved hodograph is purely linear. Growth of circulation around a supercell updraft occurs only when there is nonadvective flux of vertical vorticity into the updraft. Because there is no vertical vorticity at its edge, the Beltrami updraft has no circulation growth. Clearly, an intensifying updraft in circular shear cannot be a pure Beltrami flow, although it does acquire some Beltrami-like features.

7. EXAMPLE OF NONLINEAR CIRCULATION GROWTH

In strong unidirectional ('straight') westerly shear, an initial storm splits into severe right-moving (SR) and severe left-moving (SL) supercells. The updraft elongates along a north-south axis owing to rotationally induced propagations of its left and right edges and it splits as the center of the updraft decays owing to downward mass-induced and nonlinear splat-induced NHVPGF (Fig. 5; K87 Fig. 3a). In simulations without Coriolis forces, the supercells are mirror images of each other with the SR (SL) updraft rotating cyclonically (anticyclonically) in the northern hemisphere. A midlevel north-south vortex pair straddles each updraft as a result of the updraft drawing up loops of the northerly environmental vortex lines (K87 Fig. 3b). According to the concept of rotationally induced propagation, the upward nonlinear spin-induced NHVPGF (or "vortex suction") beneath these vortices should propagate the south (right) edges of both updrafts southward and the north (left) edges northward with little across-shear propagation of the centroids, although the outward propagations would be opposed to some extent by inward advection associated with convergent flow. There is no mechanism for the split storms to continue moving away from each other. The storm structures would once again resemble that in Fig. 5. In response to the outward propagation of both left and right edges, the updrafts would elongate and split again. Storm splitting would be cyclical.

In actuality, the vortex suction is responsible only for the outward propagation of the right edge of the right-moving updraft and the left edge of the left-moving updraft with the opposite edges propagating inward through mass- and nonlinear splat-induced propagation dominating the rotationally induced propagation (Fig. 6; DJ02). This arrangement allows the updraft centroid of the SR (SL) storm to propagate rightward (leftward). In contrast to the initial storm, vortex suction is important only on one side of the supercells. Linear shear-induced propagation acts on the east and west edges of the updrafts and at each level opposes advection of the edges by the environmental storm-relative wind. It thus resists the shearing over of the updrafts (RK82), but plays no part in across-shear propagation.

Now consider how the right-moving supercell continues to rotate and propagate rightward long after the split. The rightward propagation of both the right and left edges of the updraft causes the cyclonic vortex to move inward towards the updraft center and the anticyclonic vortex to move outward towards the downdraft. The cyclonic vortex stays on the south side of the updraft center because it too propagates (owing to tilting and subsequent vertical stretching of environmental vorticity on the south flank). The updraft gains cyclonic circulation because, by means of its edge propagation, it takes in cyclonic vorticity at its south edge and sheds anticyclonic vorticity at its north edge. On the southeast edge the nonlinear vortex suction is large and gives rise to the strong rotationally induced propagation to the right needed to move this edge rightward and overcome leftward advection of this edge associated with flow converging into the updraft. On the northwest edge the nonlinear vortex suction only reduces the downward mass-induced and nonlinear splat-induced NHVPGFs that decay the updraft on this side. The mass- and splat-induced propagations and advection by the deviation wind move this edge rightward by dominating the leftward spin-induced propagation. At 40 min in WR's simulation, increases in circulation around the edge arise mostly from the product of strong upward nonlinear NHVPGF and cyclonic vorticity on the south side. By 80 min, the negative nonlinear NHVPGF on the SR updraft's north edge has become comparable with the positive one on the southeast edge. Thus the splat-induced decay and shedding of anticyclonic vorticity at the updraft's trailing edge eventually may become as significant as the rotationally induced propagation and ingestion of cyclonic vorticity at its leading edge.

In summary, the rotationally induced NHVPGF plays the dominant role in the early maintenance, rotation, and propagation of supercells in straight shear with one exception. It cannot account for the decay and resulting inward propagation of the updrafts' trailing edges

Why is the SR storm generally the stronger storm? Firstly, Coriolis effects on the storm make the cyclonically rotating updraft a little stronger than the anticyclonically rotating left-moving updraft (Klemp and Wilhelmson 1978). Stretching of planetary vorticity in convergent flow increases (decreases) the rotation of the cyclonic (anticyclonic) updraft. This positive increase in ζ together with inclusion of planetary vorticity increases (decreases) the spin forcing of pressure in the cyclonic (anticyclonic) vortex. [Recall from Section 4 that this forcing is $-\rho_s\left(f\zeta + \omega' \bullet \omega'/2\right)$.] Consequently, the cyclonic vortex has a lower pressure and larger vortex suction beneath it. This results in greater (lesser) propagation of the leading (trailing) edge of the SR (SL) updraft and hence more accumulation (less shedding) of cyclonic vorticity. Thus the SR updraft is slightly stronger, rotates faster and propagates a little further off the hodograph than the SL updraft. However, a second effect, hodograph curvature, imparts a larger bias (Klemp and Wilhelmson 1978). In observed cases of nearly unidirectional shear, the hodograph is not straight close to the ground. The shear vector generally turns clockwise from 0 to 2 km owing to the Ekman layer and warm-air advection (Coriolis effects on the environment). In such cases the rightward propagation is still predominantly nonlinear but linear NHVPGFs in the lowest 2 km provide the bias that favors the SR storm (WR).

8. CONCLUSIONS

The local motion of the updraft edge normal to itself is the vector sum of advection by the local wind and propagation caused by the net vertical force, which is the NHVPGF in inviscid anelastic flow. The local propagation velocity of the edge along its outward normal is equal to the vertical force divided by the gradient of vertical velocity along the inward normal. Circulation around an updraft perimeter gains at a rate equal to the line integral around the edge of vertical vorticity times the outward local propagation velocity. In other words, an updraft edge develops cyclonic circulation around it by propagating outwards (inwards) on its cyclonic (anticyclonic) side. Equivalently, the updraft increases its rotation by ingesting cyclonic vorticity and shedding anticyclonic vorticity.

In straight shear, circulation growth and anomalous propagation of the updraft's leading edge are nonlinear, as deduced by Rotunno and Klemp (1985) and WR. In the right-moving supercell in circular shear, the cyclonic vortex is close to but to the right of the updraft center where its nonlinear suction helps to maintain the updraft. The smaller anticyclonic vortex is on the left updraft edge. Rightward propagation is predominantly linear and associated with upward

NHVPGF on the right edge and downward linear NHVPGF on the left edge. Circulation growth is also linear because the updraft edge propagates linearly outward on its cyclonic side and linearly inward on its anticyclonic side. In circular shear, nonlinear NHVPGF is upward around the whole edge at 3 km and increases updraft radius and intensity. However, its contributions to rightward centroid propagation and to the growth of circulation are minor.

According to WR, the two commonly accepted paradigms of updraft rotation and propagation are the nonlinear 'vertical-wind-shear paradigm' and the quasi-linear 'helicity paradigm'. Weisman and Rotunno concluded that the 'vertical-wind-shear' viewpoint applied to all supercells regardless of the type of environmental shear. In contrast, DJ02 concluded, based on the across-shear propagation of updraft maxima being nonlinear in straight shear and mostly linear in circular shear, that there are two partial paradigms of supercell behavior rather than one all-inclusive model. The present investigation shows that the mechanism for the growth of circulation around updraft perimeters also proceeds in keeping with the vertical-wind-shear viewpoint in straight shear and in accordance with the helicity perspective in circular shear. Like propagation, development of rotation in supercells depends on hodograph shape.

Acknowledgments. This work was supported in part by NSF grants ATM-0003869 and ATM-0004526.

9. REFERENCES

Davies-Jones, R., 2002a: Linear and nonlinear propagation of supercell storms. *J. Atmos. Sci.,* **59**, 3178-3205.

Davies-Jones, R., 2002b: Linear and nonlinear propagation of supercell storms. *Preprints,* 21st Conf. Severe Local Storms, San Antonio, TX, Amer. Meteor. Soc., 511-514.

Davies-Jones, R., 2004: Growth of circulation around supercell updrafts. *J. Atmos. Sci.,* (in press).

Klemp, J. B., 1987: Dynamics of tornadic thunderstorms. *Annu. Rev. Fluid Mech.*, **19**, 369-402.

Klemp, J. B., and R. B. Wilhelmson, 1978: Simulations of right- and left-moving storms produced through storm splitting. *J. Atmos. Sci.,* **35**, 1097-1110.

Lemon, L. R., 1976: Wake vortex structure and aerodynamic origin in severe thunderstorms. *J. Atmos. Sci.,* **33**, 678-685.

Rotunno, R., and J. B. Klemp, 1982: The influence of the shear-induced pressure gradient on thunderstorm motion. *Mon. Wea. Rev.*, **110**, 136-151.

Rotunno, R., and J. B. Klemp, 1985: On the rotation and propagation of simulated supercell thunderstorms *J. Atmos. Sci.,* **42**, 271-292.

Stewart, H. J, 1945: Kinematics and dynamics of fluid flow. *Handbook of Meteorology*, McGraw-Hill, 411-500.

Weisman, M. L., and R. Rotunno, 2000: The use of vertical wind shear versus helicity in interpreting supercell dynamics. *J. Atmos. Sci.,* **57**, 1452-1472.